JACS
JOURNAL OF THE AMERICAN CHEMICAL SOCIETY
Article
pubs.acs.org/JACS

D-Amino Acid Scan of Two Small Proteins

Mark D. Simon,[†] Yuta Maki,[†,‡] Alexander A. Vinogradov,[†] Chi Zhang,[†] Hongtao Yu,[§] Yu-Shan Lin,[§] Yasuhiro Kajihara,[‡] and Bradley L. Pentelute*[,†]

[†]Department of Chemistry, Massachusetts Institute of Technology, 77 Massachusetts Avenue, Cambridge, Massachusetts 02139, United States

[‡]Department of Chemistry, Graduate School of Science, Osaka University, 1-1, Machikaneyama-cho, Toyonaka, Osaka 560-0043, Japan

[§]Department of Chemistry, Tufts University, 62 Talbot Avenue, Medford, Massachusetts 02155, United States

Supporting Information

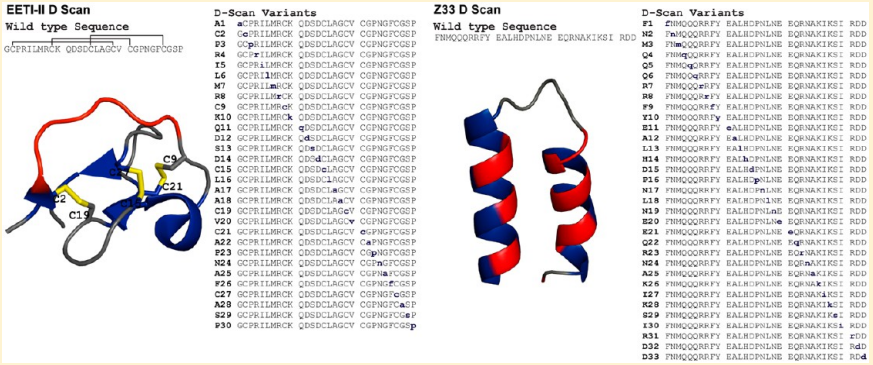

ABSTRACT: A "D-scan" of two small proteins, the disulfide-rich *Ecballium elaterium* trypsin inhibitor II (EETI-II) and a minimized Z domain of protein A (Z33), is reported. For each protein, the stereochemistry of one amino acid at a time was inverted to generate a series of diastereomers. In much the same way an alanine scan determines necessary residues for protein function, the D-scan elucidated the critical stereocenters of the 30-residue EETI-II and the 33-residue Z33. The folding properties and activity of each variant were investigated. A total of 24 out of 30 EETI-II D-scan analogues folded to give a three-disulfide product. Of the 24 variants that folded, half were high-affinity trypsin inhibitors, and three were as active as the wild type (WT). Of these 12 active variants, most were substantially less stable to reduction than WT EETI-II (WT first reduction potential −270.0 ± 1.5 mV, WT second reduction potential −307.2 ± 1.1 mV). Similarly, ten Z33 analogues retained high binding affinity to IgG (K_D < 250 nM, WT: 24 ± 1 nM) and 12 additional analogues had reduced but appreciable IgG binding affinity (K_D between 250 nM and 2.5 μM). As with EETI-II, most Z33 analogues were substantially less stable than the WT ($\Delta G(H_2O, 263\ K)$ = 2.4 ± 1.2 kcal/mol). Collectively, our findings show that the D-scan is powerful new strategy for studying how the stereochemistry of amino acids affects the structure and function of proteins.

INTRODUCTION

Nature is chiral. Biopolymers from DNA to lipids are handed, as are many small-molecule natural products. But while Nature uses multiple isomers of some products, such as carbohydrates and steroids, natural proteins are homochiral polymers, composed exclusively of L-amino acids.[1−3] There are post-translational amino acid isomerases and non-ribosomal synthases that produce short peptides with D-amino acids, but such enzymes are uncommon.[4−6] Why does nature avoid extensive use of genetically encoded D-amino acids or post-translational epimerases? In principle, using D-amino acids in a protein would allow access to a broader folding and structural space.[7] Research has shown rational substitution of D-amino acids for glycine in a favorable confirmation can improve thermal stability,[7,8] and targeted insertions elsewhere can improve stability toward proteases.[9] Further, D-scans of several bioactive peptides have shown them to be tolerant of D-amino acid substitutions, with some constructs having enhanced biological properties.[10−14]

To investigate the effect of introducing D-amino acids into existing proteins, we selected two proteins, *Ecballium elaterium* trypsin inhibitor II (EETI-II) and a minimized Z domain of protein A (Z33),[15] and prepared two series of diastereomers by inverting a single amino acid in each analogue (Figure 1). For achiral glycine residues, we substituted D-alanine, as it is hypothesized that glycine is Nature's placeholder for D-amino acids.[7,8] Like alanine scans used to determine which side chains are important for function and folding, this "D-scan" identified the important chiral centers for folding and activity of EETI-II

Received: April 20, 2016
Published: August 5, 2016

DOI: 10.1021/jacs.6b03765
J. Am. Chem. Soc. 2016, 138, 12099−12111

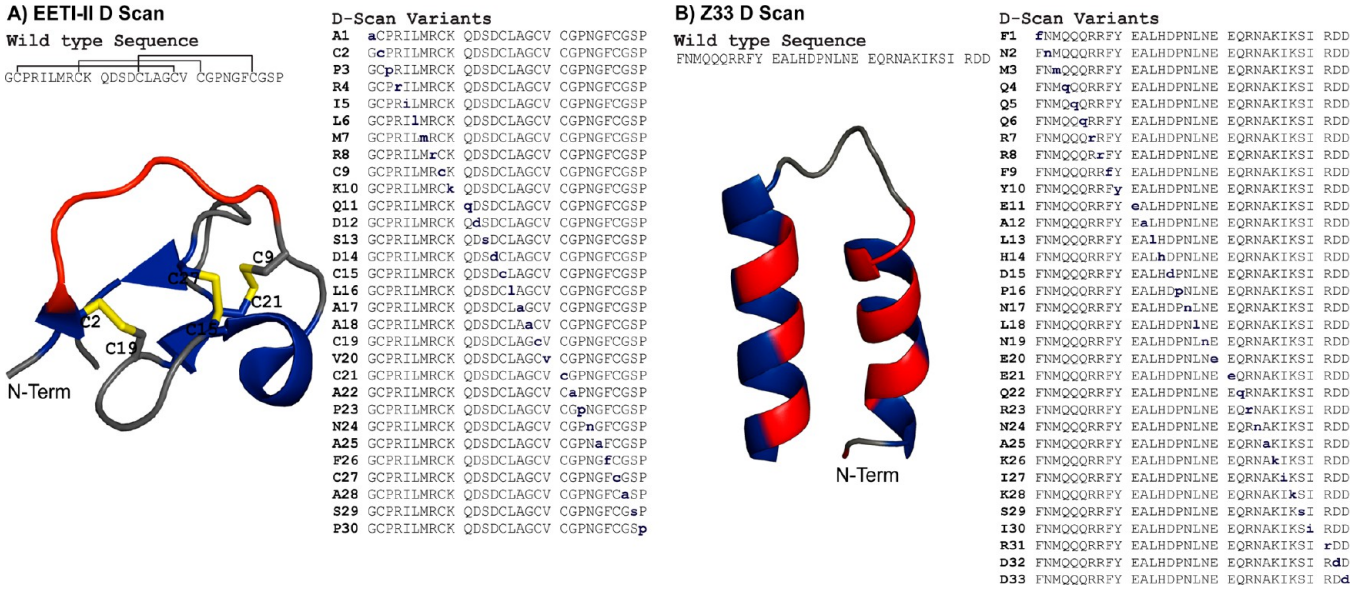

Figure 1. Illustration of the D-scan of EETI-II and Z33. Amino acids represented by black capital letters are L-amino acids, and amino acids represented by blue lower case letters are D-amino acids. The name of each analogue is the substituted D-amino acid and its position. (A) D-scan of EETI-II. In the wild type sequence of EETI-II, disulfide connectivity is shown with black lines. In the cartoon representation of EETI-II, constructed in PyMOL from crystallographic data reported by Kraetzner et al.,[35] the disulfide bridges are yellow, the trypsin binding loop is red, secondary structure annotated in the PDB is blue, and the remaining regions are gray. (B) D-scan of Z33. The cartoon representation of Z33 was constructed from NMR structural data reported by Starovasnik et al.,[51] amino acid residues at the binding interface with IgG are red, secondary structure annotated in the PDB is blue, and the remaining regions are gray. Binding residues were determined from the cocrystal structure of intact Z-domain and an IgG fragment.[36]

and Z33. Strikingly, most variants folded, and about a third retained binding affinity within an order of magnitude of the wild type (WT).

EETI-II is a three-disulfide cysteine knot, while Z33 is composed of two antiparallel 3.6_{13}-helices bridged by a short loop. These two proteins were selected for several reasons. First, both EETI-II and Z33 are highly representative of small protein scaffolds that are of interest in developing novel protein functionality. EETI-II-like cysteine knots have high thermal and proteolytic stability, tolerance to mutation, oral bioavailability, and low immunogenicity, making them attractive targets for therapeutic protein engineering. Several successful engineering efforts have yielded constructs that are FDA approved and used clinically.[16−24] Minimal helical scaffolds such as Z33 have also been extensively used to engineer novel biological functions.[25−28] Since α-helix interfaces are commonplace in protein−protein binding interactions, such scaffolds are routinely evolved to bind proteins, and thus to elicit biologically relevant functions.[29−31]

Second, both proteins are chemically accessible. Although there exist methods to genetically encode non-proteogenic amino acids, chemical synthesis offers a more general and robust route to proteins incorporating many different D-amino acids.[32,33] Both EETI-II and Z33 can be assembled in good yield by fast flow stepwise solid-phase peptide synthesis without the need for fragment condensation or native chemical ligation.[34] This vastly simplified synthesis and improved yields, an important consideration when undertaking the total synthesis of over 60 proteins.

Third, Native EETI-II folds by forming three disulfide bonds, and this reaction can be monitored via LC/MS.[37,38] The first and second form rapidly, giving a stable, early-eluting two-disulfide intermediate. The third disulfide then forms, locking the protein into its final knotted conformation, and yielding a chromatographically resolved, early-eluting final product.[24] The nature of the intermediate and final products can be confirmed by the loss of 2 Da per disulfide bond. Similarly, WT Z33 forms two helices, which yield a canonically helical far-UV circular dichroism (CD) spectrum.[15] Perturbations to the helical structure are observed as a loss in helicity, and an increase in random coil content.

Fourth, there is a high-resolution crystal structure of EETI-II bound to trypsin,[35] a high-resolution crystal structure of the Z-domain of protein A bound to a human IgG,[36] and an NMR structure of Z33 with five additional N-terminal residues.[39] Observed changes in the folding, structure, and function of EETI-II and Z33 can be correlated to the structure of the native proteins and their interaction with their binding partners, enabling a richer analysis of our findings. Furthermore, structural data supported molecular dynamics (MD) simulations to provide additional insight into the effect of D-amino acid substitutions.

Finally, there are facile assays available to calculate the binding affinity of EETI-II and Z33 to their corresponding targets. A chromogenic assay can be used to calculate the binding affinity of non-covalent trypsin inhibitors.[40,41] In this assay, trypsin hydrolyzes *N*α-benzoyl-Arg-(4-nitro)anilide, releasing the intensely yellow nitroaniline. The rate of increase in absorbance is proportional to the trypsin activity, and the binding affinity is determined by calculating trypsin activity in the presence of various concentrations of EETI-II.[41] As a minimized Z-domain of protein A, Z33 binds to hIgG with a nanomolar affinity, and this interaction can be monitored using biolayer interferometry methods.

RESULTS

D-Scan of EETI-II. *Synthesis and Folding of EETI-II Analogues.* Linear peptides were assembled using an improved and optimized fast flow peptide synthesis protocol (0.1 mmol scale),[42,43] affording about 100 mg of each crude analogue. Stepwise solid-phase peptide synthesis was performed on

DOI: 10.1021/jacs.6b03765
J. Am. Chem. Soc. 2016, 138, 12099−12111

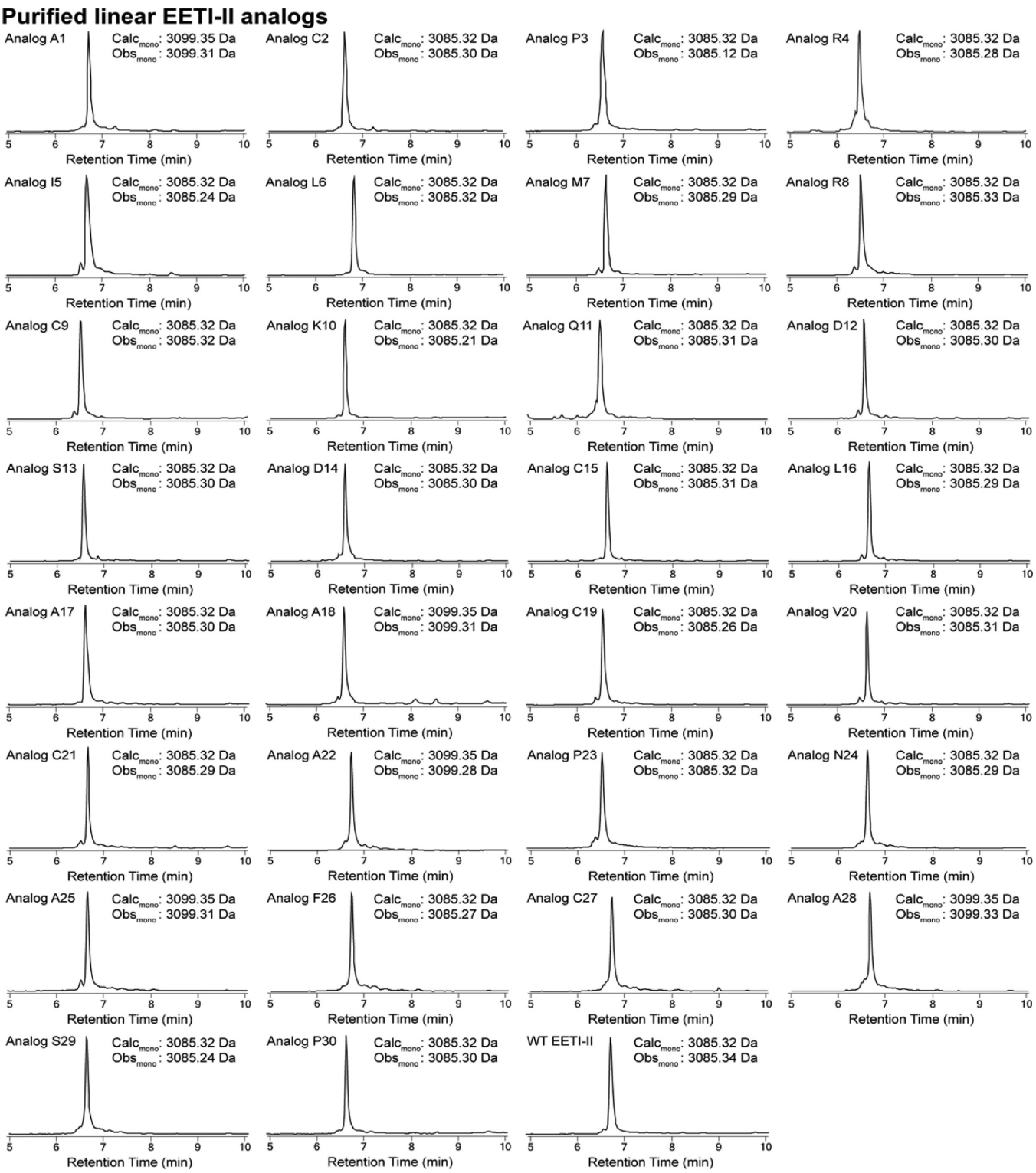

Figure 2. LC/MS analysis of pooled fractions from the RP-HPLC purifications of each linear, unfolded analogue of EETI-II. In all cases, calculated and observed masses are monoisotopic, and total ion chromatograms are shown. See SI for chromatographic conditions.

ChemMatrix Rink amide resin at 70 °C using 1-[bis-(dimethylamino)methylene]-1*H*-1,2,3-triazolo[4,5-*b*]-pyridinium 3-oxid hexafluorophosphate activation and N-terminal fluorenylmethoxycarbonyl (Fmoc) protection. Amide bond formation was allowed to proceed for 30 s, and Fmoc groups were removed in 20 s with 20% (v/v) piperidine in dimethylformamide (DMF). The total time required to incorporate an amino acid was 2 min, enabling synthesis of five analogues per day. Representative LC/MS analyses of crude peptides are shown in the Supporting Information (SI).

We next investigated folding conditions for WT EETI-II. The reduced polypeptide required 10 min to fold in a glutathione-based redox buffer,[41] and was insensitive to the concentrations of oxidized and reduced glutathione in the range we explored. In

DOI: 10.1021/jacs.6b03765
J. Am. Chem. Soc. 2016, 138, 12099−12111

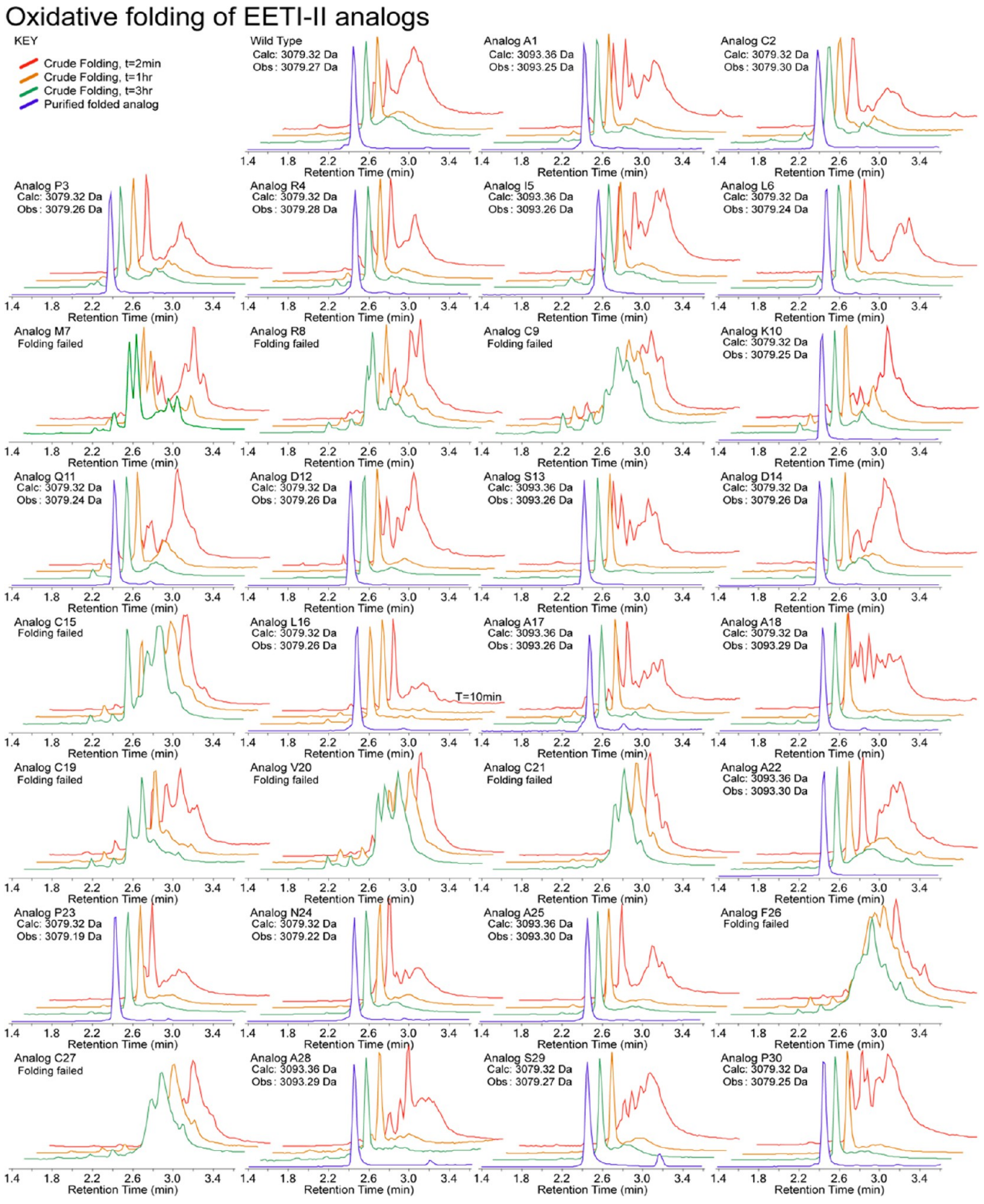

Figure 3. Time coursed folding reaction for each EETI-II analogue. Each EETI-II analogue was dissolved in a glutathione-based redox buffer (2 mM GSSG, 10 mM GSH, pH = 7.8) and the folding reaction was monitored by LC/MS, with aliquots quenched and analyzed after 2 min, 1 h, and 3 h. The formation of a product six Daltons less massive than the starting material that elutes as a single peak significantly earlier the starting material is characteristic of a successful folding reaction. Unsuccessful folding reactions generally produce a heterogeneous mixture of products that elute as a broad peak somewhere between the desired, folded product and the starting material. The desired product was isolated form all successful folding reactions by preparative RP-HPLC and the LC/MS analysis of pooled fractions is shown in blue, where applicable. In all cases, calculated and observed masses are monoisotopic, and total ion chromatograms are shown. See SI for chromatographic conditions.

cysteine/cystine redox buffer or aerated phosphate buffer, WT EETI-II folded in several hours. In an effort to drive analogues

DOI: 10.1021/jacs.6b03765
J. Am. Chem. Soc. 2016, 138, 12099−12111

toward properly folded thermodynamic products, the most reducing glutathione-based folding buffer we investigated was selected (2 mM GSSG, 10 mM GSH, 25 mM Tris, pH = 7.8).

After establishing folding conditions for WT EETI-II, we undertook analytical folding and trypsin inhibition experiments with the analogues. First, we purified several milligrams of each linear peptide via RP-HPLC (Figure 2). The purified linear peptides were then folded by dissolution to 3.3 mM in dissolving buffer (6 M guanidinium chloride, 0.2 M phosphate, pH = 6.9) and diluted to 0.33 mM with folding buffer. Folding reactions were monitored by LC/MS, with time points at 2 min, 1 h, and 3 h (Figure 3).

Under these folding conditions, 21 out of 30 analogues formed products that appeared as a single, well-defined, early-eluting peak 6 Da less massive than the starting material during LC/MS analysis. This material was deemed "folded", although it is possible that in some cases there was a mixture of co-eluting three-disulfide products. If folding was disrupted, however, an inhomogeneous mixture of products was seen. Folded three-disulfide products were isolated by RP-HPLC to afford pure material for the trypsin inhibition assay (Figure 3).

The nine analogues that failed to fold in the glutathione redox buffer were subjected to cysteine/cystine folding buffer, and oxidation with atmospheric oxygen in phosphate buffer (100 mM phosphate, pH = 8). None folded well in the cysteine-based buffer, but three gave a single, early-eluting three-disulfide product upon air oxidation. These folded products were then purified by RP-HPLC for the trypsin inhibition assay (SI, Figure S4).

Trypsin Inhibition Activity of EETI-II Analogues. With 24 folded, purified EETI-II analogues in hand, we assayed their activity against a commercial sample of bovine pancreatic trypsin.[40,41] EETI-II was diluted with 2 mM N^{α}-benzoyl-Arg-(4-nitro)anilide in trypsin buffer (60 mM Tris, 20 mM $CaCl_2$, pH = 7.8) and 80 nM trypsin in 1 mM HCl was added to give a final trypsin concentration of 4 nM. Final EETI-II concentrations of 100 nM, 32 nM, 16 nM, 8 nM, 4 nM, 2 nM, 1 nM, 500 pM, 250 pM, and 0 pM were used to obtain measurements to accurately calculate a broad range of binding affinities. The absorbance at 410 nm was monitored to track the formation of the yellow nitroaniline liberated by catalytic hydrolysis of N^{α}-benzoyl-Arg-(4-nitro)anilide. The rate of change in absorbance became linear in less than 30 min, and the reaction was monitored for a total of 3 h. Long monitoring times were necessary because a low concentration of trypsin was used to improve the sensitivity of the assay. We found binding affinities more than 5-fold lower than the trypsin concentration cannot be quantified. The rate of change in absorbance was taken as a direct measure of residual trypsin activity and used to calculate the binding affinity.[41] For each analogue, the assay was performed in quadruplicate in a 96-well plate (two analogues per plate). Representative data for four analogues of varying activity are shown in Figure 4, and the complete results are tabulated in Table 1. Of 24 analogues assayed, 12 were high-affinity trypsin inhibitors (K_D < 15 nM), and three were as active as WT EETI-II.

Thermodynamic Stability of EETI-II Analogues. To investigate the thermodynamic stability of the 12 active EETI-II analogues, the synthesis was scaled up to 0.2 mmol and each of the active variants was folded on a larger scale. The crude linear peptide was dissolved to a concentration of 3.3 mM in dissolving buffer, then slowly diluted with folding buffer to a final concentration of 0.29 mM. After 1 h, each folded analogue was isolated by preparative RP-HPLC, affording 10−20% of highly pure, folded material. This procedure was found to be higher yielding than first purifying the linear peptide, folding, and then repurifying the final product.

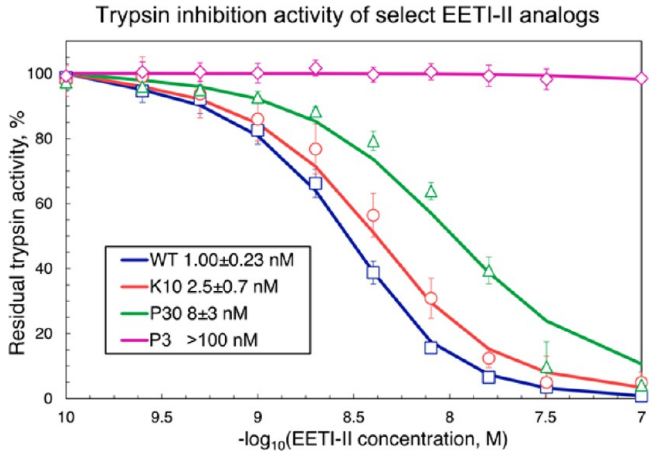

Figure 4. Representative trypsin inhibition assay results. Binding affinity was determined by incubating trypsin with various concentrations of each analogue and measuring the residual catalytic hydrolysis of $N\alpha$-benzoyl-Arg-(4-nitro)anilide, a chromogenic trypsin substrate, via the absorbance at 410 nm. This implementation of the assay is sensitive enough to differentiate a 2.5 nM binder (K10) from a 1 nM binder (WT). Errors are given as 95% confidence intervals. See SI for details of the assay and fitting procedure.

Table 1. Trypsin Affinity of EETI-II Analogues

analogue	trypsin binding (nM)[a]	analogue	trypsin binding (nM)[a]
WT	1.00 ± 0.23	L16	>100
A1	2.01 ± 0.27	A17	3.2 ± 0.8
C2	>100	A18	>100
P3	>100	C19	N/A
R4	>100	V20	N/A
I5	>100	C21	N/A
L6	>100	A22	>100
M7	>100	P23	0.92 ± 0.15
R8	>100	N24	0.92 ± 0.16
C9	N/A	A25	0.89 ± 0.13
K10	2.5 ± 0.7	F26	N/A
Q11	13 ± 5	C27	N/A
D12	3.0 ± 2.0	A28	72 ± 28
S13	3.1 ± 1.0	S29	7.3 ± 1.8
D14	11 ± 4	P30	8 ± 3
C15	>100		

[a]The trypsin binding affinity of each analogue calculated via the chromogenic trypsin inhibition assay is tabulated, with errors reported as 95% confidence intervals. Trypsin binding affinities >100 nM could not be detected, and binding affinities below 0.8 nM could not be accurately quantified. N/A indicates an analogue that failed to fold.

We then attempted to establish a melting temperature for EETI-II. The far-UV CD spectrum of WT EETI-II showed no change with temperature or urea concentration, and thermally induced conformational changes were not detected by differential scanning calorimetry. These results are not surprising because EETI-II is stabilized primarily by three disulfide bonds, with little canonical secondary structure, and similar results have been reported for another cysteine knot protein.[44] Thus, to determine the relative stability of each active EETI-II analogue, we investigated the reduction potential of the disulfide bonds using a procedure adapted from Nolan and co-workers.[45]

DOI: 10.1021/jacs.6b03765
J. Am. Chem. Soc. 2016, 138, 12099−12111

To evaluate the reduction potential, each active variant was incubated in a series of dithiothreitol-based redox buffers with potentials ranging from −240 to −390 mV. After incubation at 4 °C for 2 weeks, aliquots of each sample were quenched with acid and analyzed by RP-HPLC. For each analogue, it was observed that one disulfide bond was readily reduced, and then the second two were reduced together. The one disulfide intermediate was generally not prevalent and poorly resolved from the fully reduced product. Furthermore, we observed that the one disulfide intermediate can form from the linear peptide even in acidic media, so observed one disulfide products were integrated with the fully reduced product.

Separate midpoint potentials were determined for the two-disulfide core, and the third disulfide. Eight of 13 samples showed Nernstian behavior, while the remaining five (WT, A1, A17, N24, and A25) had not yet reached equilibrium under these conditions. After incubation at 4 °C for an additional 4 weeks, these five analogues also exhibited Nernstian behavior. Raw chromatograms for WT EETI-II and analogue D12 are shown in Figure 5, and fitted data for four analogues of varying stability are shown in Figure 6. The remaining data are in the SI. Complete results are summarized in Table 2.

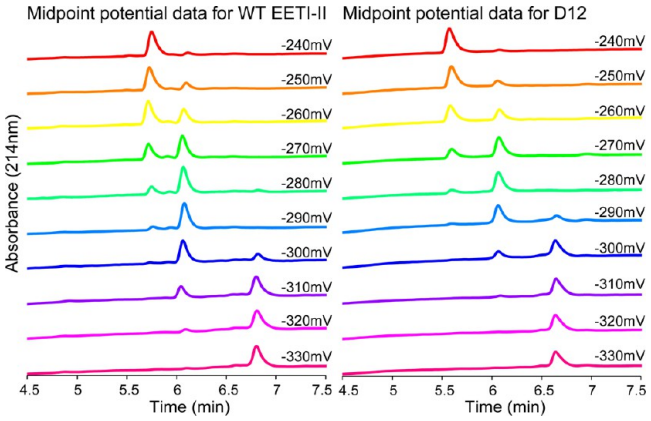

Figure 5. Raw chromatograms of WT EETI-II and analogue D12 after incubation in redox buffers of various potentials. The topmost (red) trace is after incubation in a −240 mV buffer and shows that the product is almost completely folded in both cases. The traces below are after incubation in buffers that are each 10 mV more reducing than the previous buffer, with the bottom (purple) trace showing complete reduction to the linear peptide after incubation in a −330 mV buffer. Upon inspection of the −300 and −310 mV results, D12 is seen to be less stable than WT, even before quantitative data processing.

Most of the analogues investigated were substantially destabilized. The third disulfide bond in A17, for example, was destabilized by 25 mV (1.2 kcal/mol), and the two-disulfide cores of K10, Q11, and D14 were destabilized by almost 50 mV (4.6 kcal/mol) relative to WT EETI-II. As can be seen in Table 2, the only three active analogues with both a two-disulfide core and the third disulfide comparably stable to WT EETI-II were A1, N24, and A25. Despite large differences in the stability of the analogues, however, we did not observe a clear relationship between stability and trypsin binding affinity.

Molecular Dynamics Simulations of Select EETI-II Analogues. MD simulations of WT EETI-II, and analogues A18, P23, N24, and A25 were performed to provide further insight into the effects of D-amino acid substitutions at these positions (see SI for detailed methods).[46−49] It was observed that in three out the four MD runs performed on A18, the G18a substitution

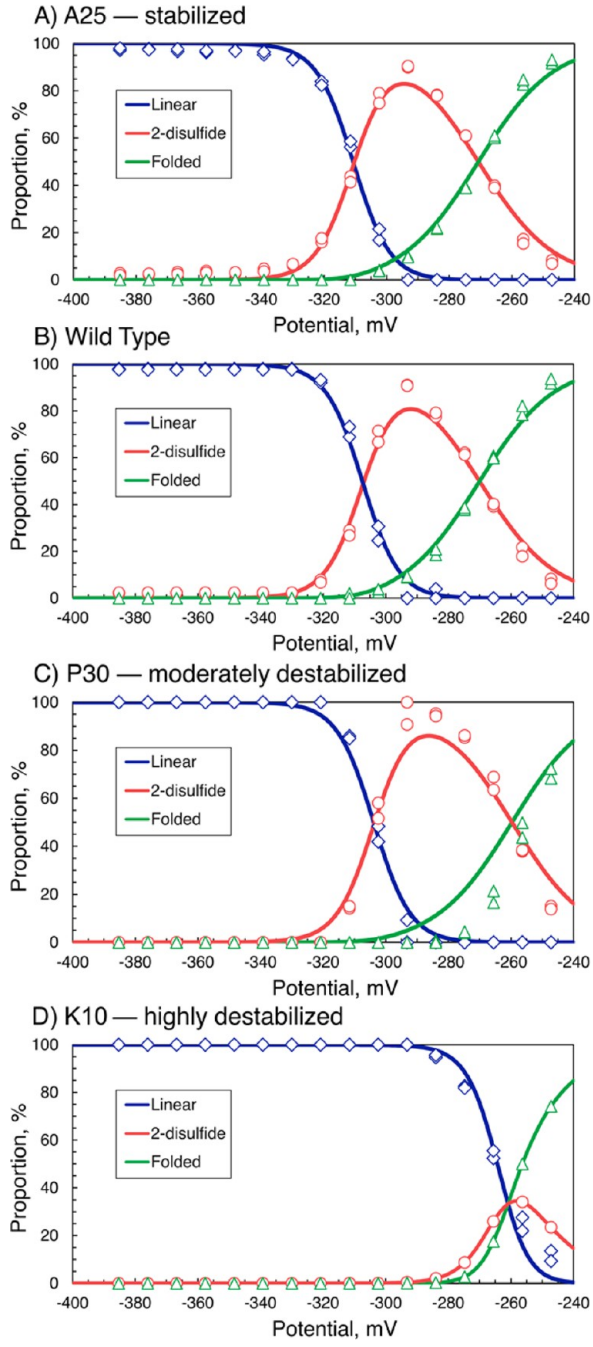

Figure 6. Representative thermodynamic data from several EETI-II analogues. The stability of each active analogue of EETI-II was determined by incubating the analogue in a series of redox buffers with potentials from −390 to −250 mV until equilibrium was achieved. Reduction potentials were calculated by fitting the equilibrium proportions of each species to the Nernst equation. In all cases, it was observed that one disulfide bond was reduced first, and then two more were reduced together. Panels A−D show the equilibrium proportion of the linear peptide, the two-disulfide intermediate, and the folded protein at various potentials for A25, WT, P30, and K10, respectively: (A) A25 is slightly more stable than WT; (B) WT; (C) P30 is less stable than WT; and (D) K10 is significantly less stable than WT.

resulted in significant deviation (RMSD) from the PDB structure (run 1 shown in Figure 7 and all runs in SI, Figure S5). In WT EETI-II, a small β sheet is formed by residues 20−22 and residues 26−28 (Figure 7A,C, left column), and the C-terminus of the peptide (residues 29 and 30) had close contacts with

DOI: 10.1021/jacs.6b03765
J. Am. Chem. Soc. 2016, 138, 12099−12111

Table 2. Reduction Potential of EETI-II Analogues

EETI-II analogue	two-disulfide core reduction potential (mV)[a]	third disulfide reduction potential (mV)[a]
WT	−307.2 ± 1.1	−270.0 ± 1.5
A1	−304.3 ± 0.4	−266.3 ± 0.9
K10	−260.9 ± 1.5	−260.9 ± 1.5
Q11	−264.1 ± 1.4	−267.1 ± 1.3
D12	−296.5 ± 1.4	−269.2 ± 1.8
S13	−293.7 ± 1.9	−273.8 ± 2.0
D14	−261.7 ± 2.5	−275.4 ± 1.6
A17	−305.6 ± 0.6	−244.7 ± 1.2
P23	−293.2 ± 1.6	−270.0 ± 2.0
N24	−304.1 ± 0.8	−266.5 ± 1.1
A25	−310.5 ± 0.9	−270.7 ± 1.3
S29	−305.1 ± 1.4	−252.9 ± 2.2
P30	−303.7 ± 1.7	−259.7 ± 2.5

[a]Reduction potentials of the two-disulfide core and third disulfide of each active EETI-II analogue were calculated by incubation in redox buffers of varying potential, and fitting the equilibrium proportions of folded protein, two-disulfide intermediate, and linear peptide to the Nernst equation. Results are tabulated here, and reported as 95% confidence intervals.

residues 18−19 (Figure 7D, left column). In the A18 analogue, the G18a mutation pushed away residues 29 and 30 toward residues 3−8 in the N-terminus (Figure 7D, right column). In runs 1 and 2 of the A18 (G18a) simulations, the original β sheet interactions between residues 20−22 and 26−28 were significantly perturbed, and new β sheet interactions formed between residues 26−27 and 7−8 (Figures 7 and S5). On the other hand, minimal structural perturbation was observed in A25 (Figure S5).

The results of the P23 and N24 analogues (three runs for each) are shown in Figure 8 and SI, Figures S6 and S7. Neither mutation seemed to disturb the structures significantly. We found that in the WT, residues 23−24 formed a type I beta turn. When P23 was mutated to p23, residues 23−24 instead adopted a type II′ beta turn; when N24 was mutated to n24, residues 23−24 formed a type II beta turn.

D-Scan of Z33. *Synthesis and Purification of Z33 Analogues.* Peptides were assembled by stepwise solid-phase peptide synthesis on 0.1 mmol ChemMatrix rink amide resin using a further improved Fast Flow peptide synthesis protocol (0.1 mmol scale),[42,43] affording about 150 mg of each crude analogue. Synthesis was performed at 90 °C using HATU activation and N-terminal Fmoc protection. Amide bond formation was allowed to proceed for 8 s, and Fmoc groups were removed in 8 s with 20% (v/v) piperidine in DMF. The total time required to incorporate an amino acid was 0.7 min, enabling synthesis of 12 analogues per day. WT Z33 and all 33 analogues were purified by RP-HPLC to yield highly pure material (Figure 9)

Binding of Z33 analogues to IgG. The IgG binding affinity of the Z33 analogues was determined via biolayer Interferometry with biotinylated trastuzumab antibody immobilized on the surface of streptavidin biosensors. Sensograms for each Z33 analogue were obtained at a series of concentrations from 156 to 5000 nM at 25 °C and fitted to obtain the dissociation constant (K_D) following the manufacturer's protocol (see SI).

As summarized in Table 3, the dissociation constant of every Z33 analogue was greater than WT Z33 (K_D = 24 ± 1 nM). Ten analogues were still potent IgG binders (K_D < 250 nM), and 12 others retained some IgG binding (K_D between 250 nM and 2.5

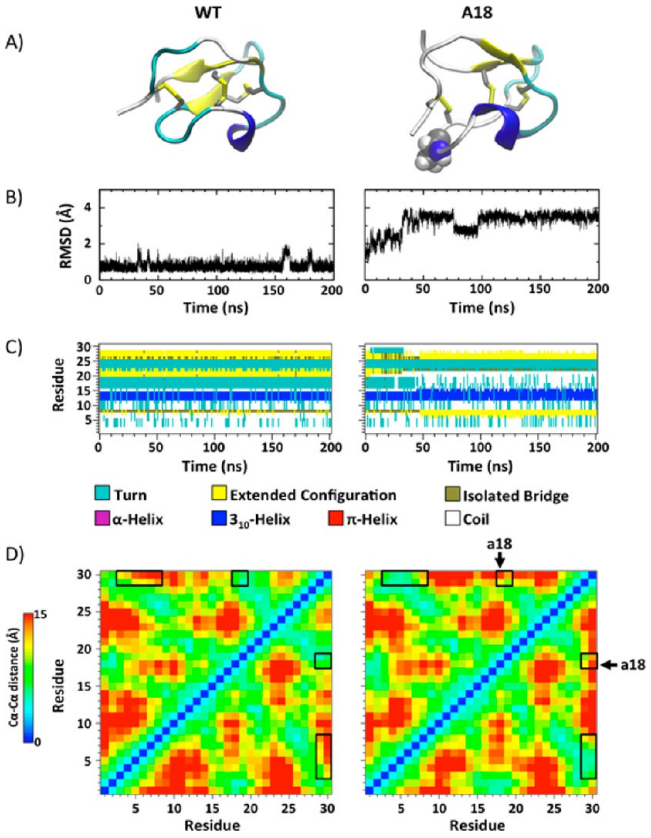

Figure 7. Molecular dynamic simulations of WT EETI-II, and analogue A18. (A) Cartoon representations of the peptide structures after 200 ns MD simulations. The structures are colored according to the secondary structure calculated using STRIDE (turn, cyan; extended conformation, yellow; isolated bridge, brown; α-helix, magenta; 3_{10}-helix, blue; π-helix, red; coil, white). The disulfide bonds are represented by sticks and the D-amino acids are highlighted with spheres. (B) Peptide backbone RMSD trajectories with respect to the PDB structure (PDB ID: 1H9H). (C) Secondary structure evolutions of each residue during the 200 ns simulations. The same color code is used as in (A). (D) Cα−Cα distance map calculated using 100−200 ns of each trajectory. Arrows denote the locations of the D-amino acids.

μM). The rest of the Z33 analogues showed little to no binding to trastuzumab. Representative data for four analogues of varying binding affinity are in Figure 10, and the remaining sensograms are in the SI.

Thermodynamic Stability of Z33 Analogues. To determine how the secondary structure of Z33 is affected by a single amino acid inversion, far-UV CD spectroscopy experiments were performed for each analogue. First, 195−260 nm CD spectra were obtained. Purified peptides were dissolved in PBS containing 30% (v/v) glycerol to a final peptide concentration of 0.2 mg/mL, and spectra were acquired at −10 °C. Glycerol prevents the buffer from freezing, and enables spectroscopy to be performed at low temperature to differentiate analogues of compromised stability. Spectra were then deconvoluted using the K2D3 algorithm to determine the α-helical content.[50] A D-amino acid in a secondary structure element may alter the spectral signature, but this was not taken into account, and the α-helicity is likely slightly underestimated for all analogues. The theoretical helicity for the WT Z33 was calculated on the basis of the solution NMR structure reported by Wells and co-workers.[51]

As summarized in Table 5, we found that every analogue was less helical than WT Z33. Five analogues (F1, M3, Q4, N17, and

DOI: 10.1021/jacs.6b03765
J. Am. Chem. Soc. 2016, 138, 12099−12111

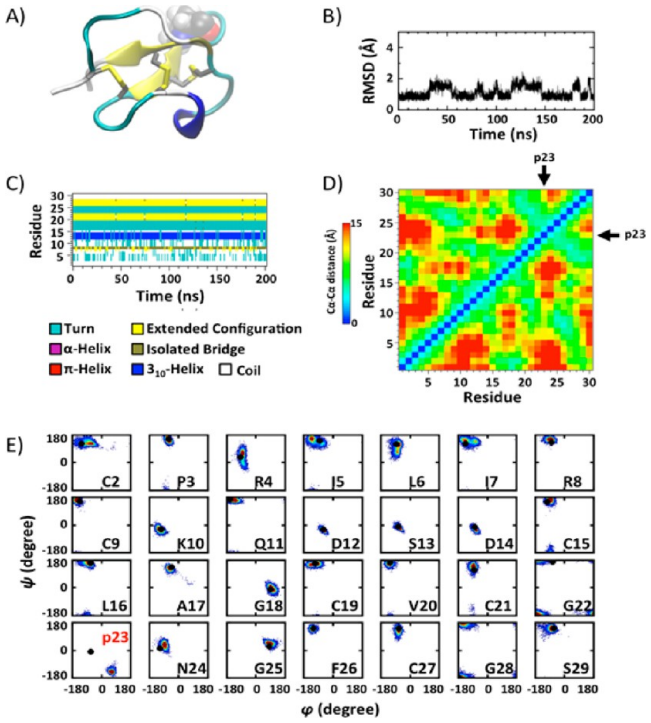

Figure 8. Molecular dynamic simulations of P23. (A) Cartoon representation of the P23 analogue structure after 200 ns MD simulations. The structure is colored according to the secondary structure calculated using STRIDE (turn, cyan; extended conformation, yellow; isolated bridge, brown; α-helix, magenta; 3_{10}-helix, blue; π-helix, red; coil, white). The disulfide bonds are represented by sticks, and the D-amino acids are highlighted with spheres. (B) Peptide backbone RMSD trajectory with respect to the PDB structure. (C) Secondary structure evolution of each residue during the 200 ns simulation. The same color code is used as in (A). (D) Cα−Cα distance maps calculated using 100−200 ns of the trajectory. Arrows denote the location of the D-amino acid. (E) Ramachandran plot for each residue calculated using 100−200 ns of the trajectory. The D-amino acid is labeled with a red lower-case letter. φ/ψ angles of the WT are shown as black dots.

R31) retained more than 90% of the wild type's helical character, while eight other analogues (R7, F9, L13, H14, P16, L18, R23, and K26) showed less than 35% α-helical character (less than half that of the WT). The remaining 20 proteins, although significantly compromised, were still substantially helical. Selected spectra from analogues with varying helical character are shown in Figure 11A, and the complete data set is in the SI.

Next, CD-aided urea denaturations of Z33 and its analogues were performed. The proteins were dissolved to 0.2 mg/mL in PBS containing 30% (v/v) glycerol and varying amounts of urea (0 to 7.5 M), and the ellipticity was measured at 220 nm and −10 °C. In 13 cases, unfolding curves appeared to extend to the regions of fully folded protein. In these cases, the resulting unfolding curves were processed assuming a two-state transition to obtain $\Delta G^{u}(H_2O, 263\ K)$ and $[urea]_{1/2}$ (see SI). Otherwise, thermodynamic parameters were not obtained; such analogues were significantly less stable than WT Z33. Figure 11B shows urea denaturations of several analogues of varying stability, and results are presented in Table 5. Complete data sets for all analogues are in the SI.

In general, urea denaturation experiments agreed with the results of spectral deconvolution, with analogues that showed little helical character melting quickly and analogues with substantial helical character melting more slowly. Of 12 proteins with complete unfolding curves, only Q4 was as stable as WT, while the other 11 analogues were less stable, both in terms of $\Delta G^{u}(H_2O, 263\ K)$ and $[urea]_{1/2}$.

DISCUSSION

D-Scan of EETI-II. The D-scan of *Ecballium elaterium* trypsin inhibitor II showed that the protein is remarkably resistant to changes in the chirality of the backbone (Figure 12). A total of 24 out of 30 analogues oxidized to give defined compounds 6 Da less massive than the starting material and significantly earlier-eluting on RP-HPLC, products we consider folded. Of the 24 analogues that folded, 12 were high-affinity trypsin binders, and 12 showed little to no activity. Of the 12 that were highly active, three were as stable as wild type, and nine were moderately to severely destabilized.

Only six of the 30 synthesized analogues failed to fold: C9, C19, V20, C21, F26, and C27. Four of these are cysteine inversions, which would intuitively be expected to directly disrupt folding by changing the position of the sulfur atoms that form disulfides. Further, F26 and V20 are adjacent to cysteine. What is surprising, however, is that all of the other analogues folded, including C2 and C15, as well as several analogues with D-amino acids adjacent to cysteine. Even analogues inverting rigid proline folded efficiently. In WT EETI-II, C2 and C15 are disulfide bonded with C19 and C27, respectively, indicating that there is significant flexibility in certain regions. Our MD simulation results of P23 and N24 suggest that although one might have expected large effects from these D-amino acid substitutions, the peptide may simply change the turn type in this region to accommodate the replacements.

All six of the mutations in the binding loop (P3-R8) abolished the inhibitory activity of EETI-II, as well as the C2 mutation adjacent to it. This result was expected on the basis of the cocrystal structure of EETI-II and trypsin, which shows a tight interaction extending from C2 to C9.[35] What was unexpected, however, was that changes far from the binding site would abolish activity, even though the analogues folded well. C15 is disulfide bonded to the binding loop, and L16 is adjacent to it, but three substitutions of D-alanine for glycine—A18, A22, and A28—also abolished activity. In these three cases, substitution of Gly with D-Ala far from the binding loop prevented efficient trypsin binding but did not disrupt folding. Substitution of D-alanine for glycine-18 is particularly interesting because it has a positive Ramachandran φ angle, which is hypothesized to indicate tolerance to substitution of D-amino acids.[7] The only other amino acid with a positive Ramachandran φ angle, A25, folded well, was a high-affinity trypsin inhibitor, and was slightly more stable than WT EETI-II.

In all cases, investigated analogues show the formation of an early-eluting two-disulfide product followed by the slower formation of a still earlier-eluting three-disulfide product. This is consistent with the known folding pathway of WT EETI-II where the C9−C21 and C15−C27 disulfides form first to generate a stable 2-disulfide core, then the C2−C19 disulfide bond forms, locking the trypsin binding loop in place. This observation does not, however, support the notion that all analogues have the native disulfide bond configuration.

Out of the analogues investigated, A1, N24, and A25 were as stable as WT and the rest were significantly destabilized. A25 has a positive φ angle, and A1 is on the N-terminus, suggesting that substitution of D-amino acids may not disrupt the conformation of the backbone. A18, the only other substitution at a residue with a positive Ramachandran φ angle, was completely inactive.

DOI: 10.1021/jacs.6b03765
J. Am. Chem. Soc. 2016, 138, 12099−12111

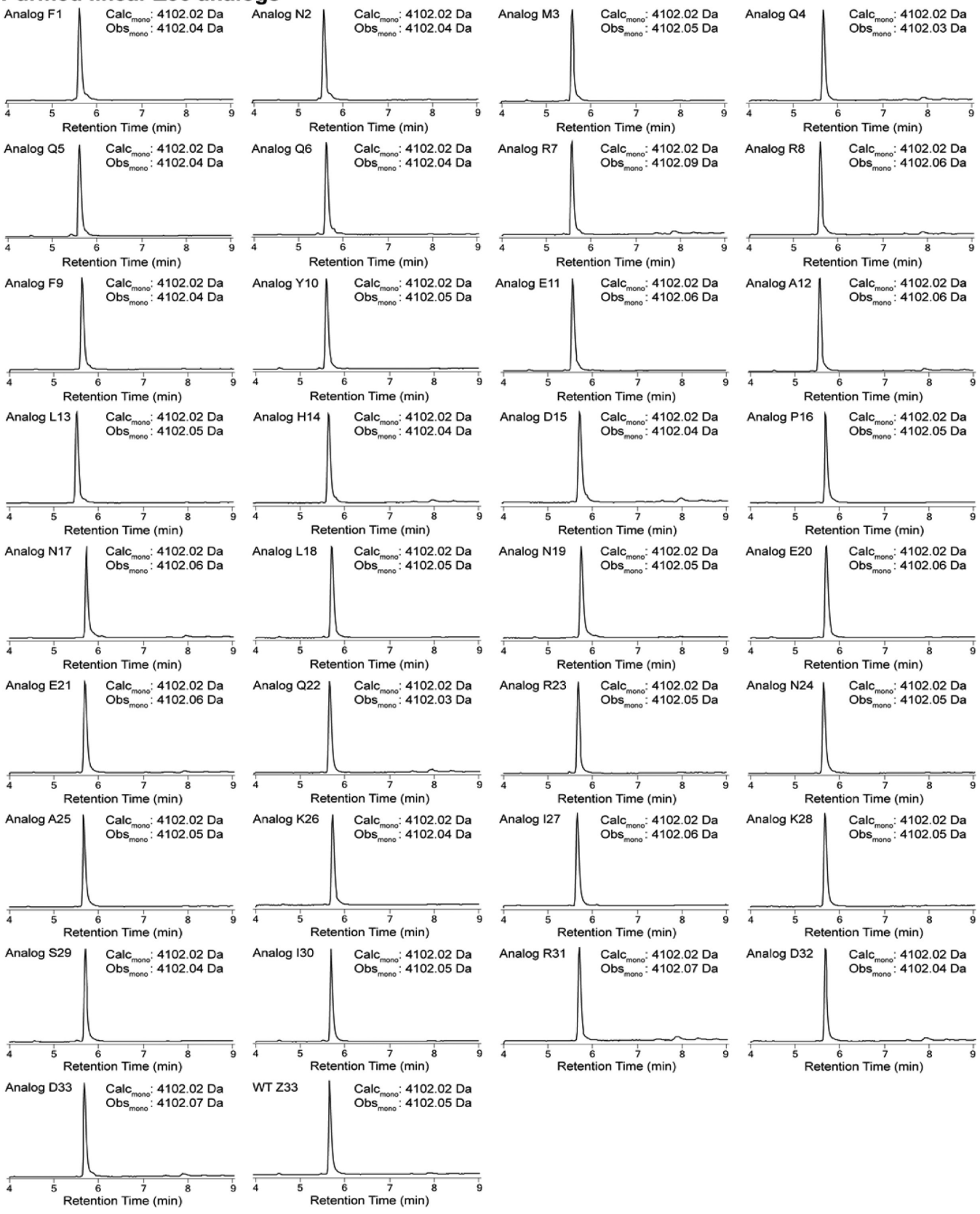

Figure 9. LC/MS analysis of pooled fractions from the RP-HPLC purifications of each Z33 analogue. In all cases, calculated and observed masses are monoisotopic, and total ion chromatograms are shown. See SI for chromatographic conditions.

Our MD simulation results suggest that the G18a mutation in A18 pushed away residues 29 and 30 toward residues 3−8 in the N-terminus, resulting in perturbation of the native β sheet interactions between residues 20−22 and 26−28 and formation

DOI: 10.1021/jacs.6b03765
J. Am. Chem. Soc. 2016, 138, 12099−12111

Table 3. Binding Constants of Z33 Analogues

Z33 analogue	K_D, μM[a]	Z33 analogue	K_D, μM[a]
WT	0.024 ± 0.001	N17	0.10 ± 0.01
F1	0.125 ± 0.005	L18	1.2 ± 0.5
N2	0.28 ± 0.03	N19	1.5 ± 0.6
M3	0.088 ± 0.003	E20	0.060 ± 0.002
Q4	0.029 ± 0.002	E21	0.083 ± 0.005
Q5	0.51 ± 0.09	Q22	0.19 ± 0.5
Q6	4 ± 2	R23	>5
R7	>5	N24	5 ± 2
R8	0.25 ± 0.04	A25	0.25 ± 0.07
F9	>5	K26	1.2 ± 0.2
Y10	>5	I27	4 ± 1
E11	0.7 ± 0.3	K28	1.2 ± 0.2
A12	1.8 ± 0.5	S29	0.056 ± 0.001
L13	>5	I30	>5
H14	2.4 ± 0.2	R31	2.2 ± 0.8
D15	1.79 ± 0.09	D32	0.036 ± 0.002
P16	3 ± 2	D33	0.030 ± 0.002

[a]Standard errors are given.

of new β sheet interactions between residues 26−27 and 7−8. Since residues 2−8 participate in the binding to trypsin, perturbation of these residues likely affects the binding greatly. In contrast, the G25a substitution in A25 led to minimal structural perturbation. Therefore, although both G18 and G25 have a positive φ angle and may be considered potential placeholders for D-amino acids, the small size of glycine at G18 might also play an important role in the structure and function of EETI-II.

Inversion of prolines 23 and 30 resulted in folded, active diastereomers of EETI-II, suggesting EETI-II is much more tolerant of disruption of proline than most proteins.[52] Surprisingly both were only moderately destabilized. The two-disulfide core of P23 is about 15 mV less stable than WT, with the third disulfide unaffected presumably because P23 is in the core of the protein. Interestingly, however, inversion of P30 has a minimal effect on the core of the protein, but destabilizes the third disulfide by 10 mV. The third disulfide, putatively between C2 and C19, would seem less likely than the core to be effected by changes to the C-terminus, suggesting that the disulfide bond configuration may be different in P30 than WT-EETI-II. Inversion of S29 shows the same trend with even greater (18 mV) destabilization of the third disulfide. The last analogue with a significantly destabilized third disulfide, A17, is the active mutation closest to C19. As there is not currently a reliable, high-throughput method to map disulfide bonds in proteins, in-depth structural analysis will be the subject of future work.[35,37,53,54]

D-Scan of Z33. The D-scan of Z33 showed that it also had significant tolerance to D-amino acid substitution. Although no analogues as active as WT Z33 were found, 22 of the 33 analogues still bound to IgG, and of these, 10 were high-affinity IgG binders with K_D < 250 nM.

Of the 11 analogues with abolished binding, 10 (Q6, R7, F9, Y10, L13, P16, R23, N24, I27, I30, R31) were located either on

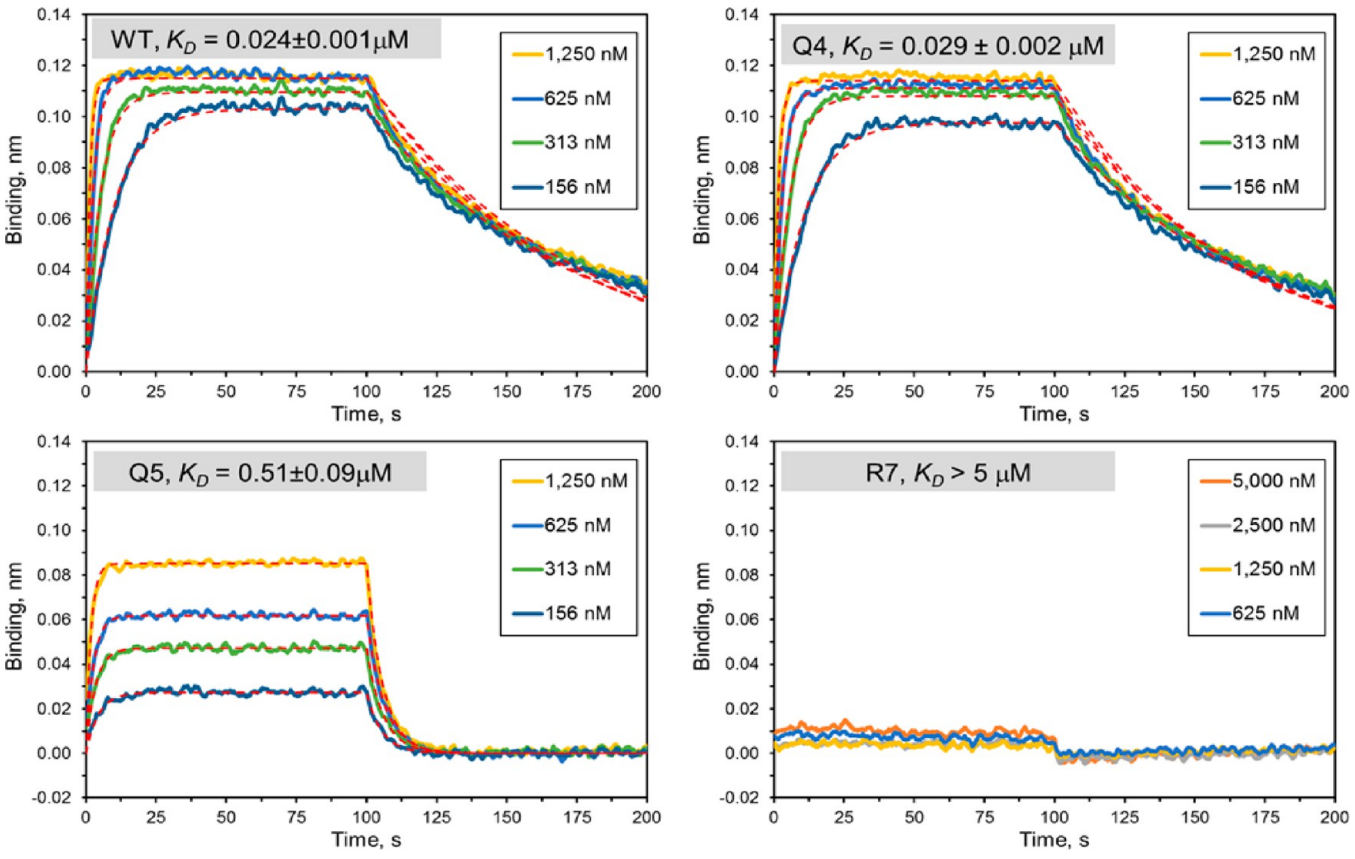

Figure 10. Representative sensograms from Z33 and several representative analogues. The IgG binding affinity of each analogue of Z33 was determined using biolayer interferometry. Streptavidin biosensors loaded with biotinylated trastuzumab antibody were sampled against Z33 variants in solution. The concentrations of Z33 variants used are shown in the legend of each sensorgram. WT Z33 had a K_D of 24 ± 1 nM, Q4 had a comparable K_D of 29 ± 2 nM, Q5 had a decreased K_D of 0.51 ± 0.09 μM, and R7 did not associate with the biosensor even at a concentration of 5 μM.

DOI: 10.1021/jacs.6b03765
J. Am. Chem. Soc. 2016, 138, 12099−12111

Table 5. Thermodynamic Stability of Z33 Analogues

analogue	$\Delta G(H_2O, 267\ K)$, kcal/mol	$[urea]_{1/2}$, M	helicity, %
WT	2.4 ± 0.7[a]	3.2 ± 1.2	67
F1	1.7 ± 0.6	2.8 ± 1.3	62
N2	1.1 ± 0.4	2.7 ± 1.2	44
M3	1.8 ± 0.6	2.6 ± 1.0	65
Q4	2.3 ± 0.8	3.5 ± 1.7	64
Q5	1.5 ± 0.4	2.6 ± 0.9	41
Q6	N.D.[b]	N.D.	43
R7	N.D.	N.D.	33
R8	1.4 ± 0.4	2.4 ± 1.0	44
F9	N.D.	N.D.	32
Y10	N.D.	N.D.	53
E11	N.D.	N.D.	36
A12	N.D.	N.D.	37
L13	N.D.	N.D.	31
H14	N.D.	N.D.	28
D15	N.D.	N.D.	38
P16	N.D.	N.D.	11
N17	1.9 ± 0.8	2.4 ± 1.4	61
L18	N.D.	N.D.	31
N19	N.D.	N.D.	38
E20	1.5 ± 0.3	2.5 ± 0.6	57
E21	1.5 ± 0.5	2.1 ± 0.8	46
Q22	N.D.	N.D.	45
R23	N.D.	N.D.	19
N24	2.3 ± 0.4	2.6 ± 0.7	47
A25	N.D.	N.D.	46
K26	N.D.	N.D.	22
I27	N.D.	N.D.	38
K28	N.D.	N.D.	42
S29	1.4 ± 0.4	2.6 ± 1.1	54
I30	N.D.	N.D.	53
R31	1.5 ± 0.2	2.5 ± 0.4	61
D32	N.D.	N.D.	52
D33	1.9 ± 0.6	3.1 ± 1.2	49

[a]Data are 95% confidence intervals. [b]N.D. = not determined.

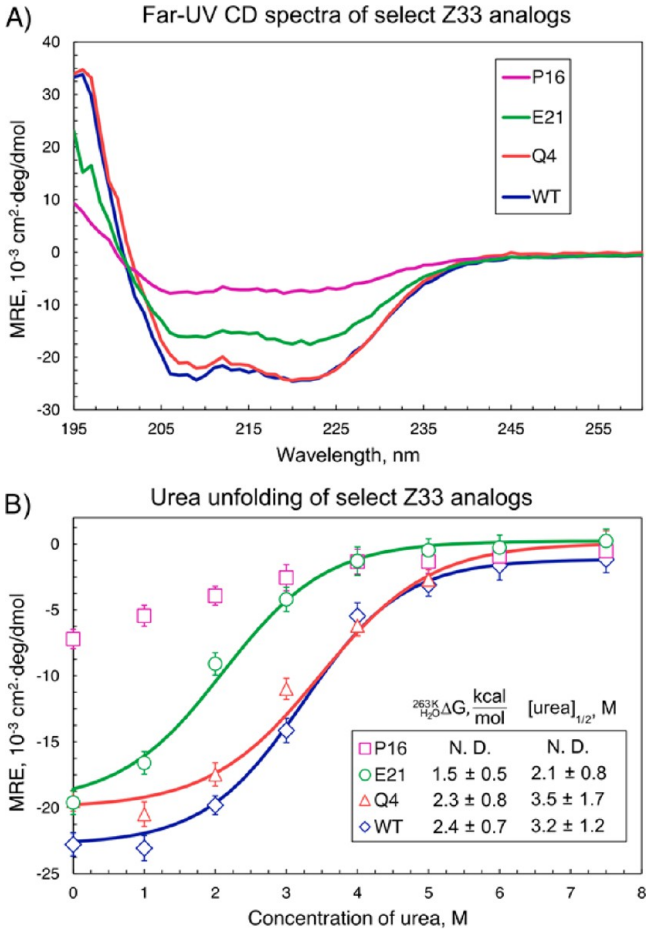

Figure 11. CD spectra and urea denaturations of select Z33 analogues. (A) 195−260 nm CD spectra were obtained for 0.2 mg/mL protein solutions in PBS with 30% (v/v) glycerol at −10 °C. (B) Mean molar ellipticity was monitored at 220 nm for 0.2 mg/mL protein solutions in PBS with 30% (v/v) glycerol and variable amounts of urea at −10 °C. Points on the plot are data points, lines are fit curves. The data were fit as described in detail in the SI, and 95% confidence intervals for $\Delta G^u(H_2O,$ 263 K) and $[urea]_{1/2}$ were calculated on the basis of the fit parameters.

the binding face of the helix or adjacent to it, confirming the importance of these residues for the binding of Z33 to IgG (Figure 13). The 11th inactive analogue is P16. As expected, inversion of the rigid proline in the loop connecting the two helices abolished activity, possibly by disrupting their intramolecular organization, which is known to be essential.[15,52]

The helical structure of Z33 analogues was found to be correlated to IgG binding (Figure 14). The eight analogues that showed significantly decreased α-helicity (R7, F9, L13, H14, P16, L18, R23, and K26) also had significantly decreased binding affinity. Four of these analogues (R7, F9, L13, and R23) did not bind to IgG, and the rest (H14, P16, L18, and K26) had binding affinities more than 40 fold lower than WT. Analogues that retained binding affinity comparable to WT (K_D < 250 nM) (F1, M3, Q4, N17, E20, E21, Q22, S29, D32, and D33) also largely retained WT helicity, with the least helical analogue being Q22 (45% helicity, 67% retained vs WT). Three analogues, Y10, I30, and R31, were highly helical but poor IgG binders. All of these mutations are located directly on the binding face of the helix, and the positions of side chains at these sites are likely essential for Z33 to bind IgG.

CONCLUSION

In conclusion, this work paves the way for detailed investigation of the role of chirality in protein folding and function. For the first time, the effect of inversion of each chiral center in a protein has been systematically studied, showing both EETI-II, a disulfide cross-linked cysteine knot, and Z33, two canonical α-helices, to be remarkably tolerant to changes in stereochemistry. In both proteins, mutations at the binding interfaces abolished activity, but many other analogues retained appreciable binding affinity.

We did not, however, find evidence to support the hypothesis that glycine acts as an achiral placeholder for D-amino acids. Substitution of D-alanine for glycine abolished activity or reduced stability in most cases. However, the only case in which substitution of a D-amino acid improved stability and retained native activity was substitution of D-alanine at glycine-25 in EETI-II. This indicates that the effect of D-amino acid substitution in proteins is more complex than previously hypothesized, and D-scans of additional proteins are needed to further elucidate the effect of D-amino acids substitutions in proteins.

So why does Nature not make extensive use of D-amino acids in higher organisms? Taken together, these results begin to offer

DOI: 10.1021/jacs.6b03765
J. Am. Chem. Soc. 2016, 138, 12099−12111

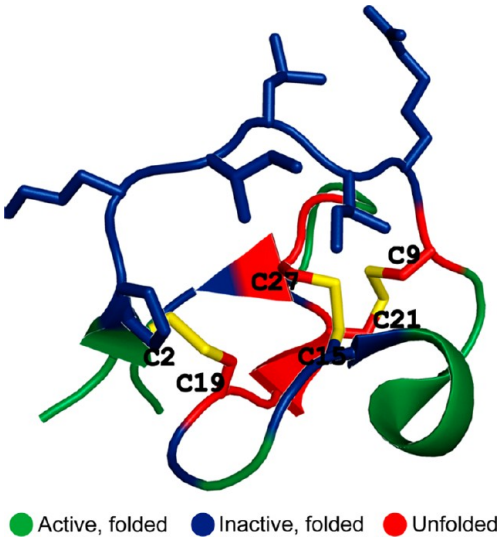

Figure 12. Graphical summary of folding and activity of EETI-II analogues. Highlighted regions show where inversion of stereochemistry resulted in analogues that did not fold (red), folded but were inactive (blue), and folded with retention of trypsin inhibition activity (green). Disulfide bonds are shown in yellow. Note that most analogues that did not fold (red regions) are mutated near disulfide bonds and most analogues that folded but did not bind (blue regions) are in the binding loop. The graphic was created with PyMOL using structural data for WT EETI-II reported by Krätzner et al.[35]

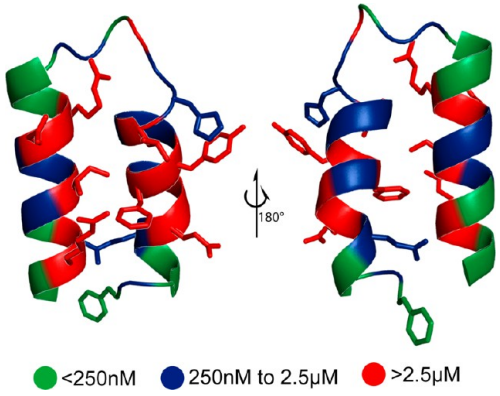

Figure 13. Graphical summary of folding and activity of Z33 analogues. Highlighted regions show where inversion of stereochemistry resulted in analogues that did not bind IgG (red, K_D > 2.5 μM), bound IgG weakly (blue, 250 nM > K_D > 2.5 μM), and retained high-affinity IgG binding (green, K_D < 250 nM). Side chains are displayed for residues at the binding interface, as determined from the co-crystal structure of intact Z-domain and an IgG fragment.[36] Note that most analogues that did not bind (red regions) are mutated at or near the binding face. The graphic was created with PyMOL using reported structural data.[51]

some insight. We found that single point inversions, like other mutations, are generally harmful or of no consequence. No analogues were identified that were significantly more active than the WT proteins, but about 35% retained high activity. In contrast to mutations from one L-amino acid to another, which arise randomly and may be accumulated until an improved multipoint mutant arises, inversion of an amino acid requires either a posttranslational epimerase or non-ribosomal synthase. This complex machinery is difficult to evolve and unlikely to be retained without conferring a significant benefit. If advantageous single point inversions are in fact rare, it may be extremely

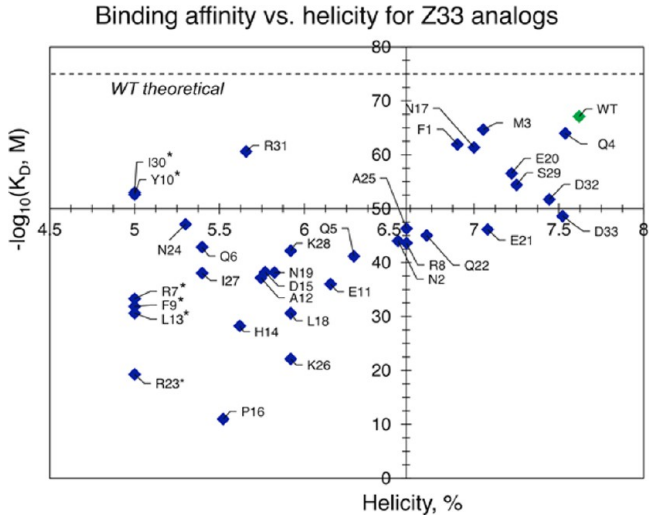

Figure 14. Binding affinity vs helicity of Z33 analogues. The helical character of the analogues was estimated via K2D3 deconvolution[50] of their 195−240 nm CD spectra, and the values for K_D are those obtained from bilayer experiments. Analogues marked with an asterisk (*) did not bind IgG under the experiment conditions; such analogues are arbitrarily assigned high K_D values of 10^{-5} M to demonstrate the overall trend. The theoretical WT helicity character is calculated from the corresponding NMR structure.[51]

difficult for potentially more beneficial proteins with multiple inversions to evolve from homochiral precursors.

Protein engineering efforts, however, can incorporate an unlimited number of D-amino acids into known or novel proteins to generate mutants with several inversions. Targeted insertions of D-amino acids could stabilize proteins against proteolysis, abolish undesired functions, and change the metabolites of degraded proteins. Such constructs are likely to be particularly useful for knottins and other highly stable proteins that can be somewhat destabilized without compromising the overall structure and function.

We believe the D-scan can be leveraged to identify cases where a protein can accept a D-amino acid without greatly affecting its function or folding, and inform efforts to engineer mixed chirality proteins with novel properties.

■ ASSOCIATED CONTENT

Supporting Information

The Supporting Information is available free of charge on the ACS Publications website at DOI: 10.1021/jacs.6b03765.

Detailed experimental procedures and complete data sets for the midpoint potential determination and trypsin inhibition assay (PDF)

■ AUTHOR INFORMATION

Corresponding Author

*blp@mit.edu

Notes

The authors declare no competing financial interest.

■ ACKNOWLEDGMENTS

This work was supported by MIT startup funds for B.L.P., the MIT Deshpande Center, and the Defense Advanced Research Projects Agency (Award No. 023504-001, B.L.P.). The support from a Tufts start-up fund and the Knez Family Faculty

DOI: 10.1021/jacs.6b03765
J. Am. Chem. Soc. 2016, 138, 12099−12111

Investment Fund for Y.-S.L. is gratefully acknowledged. A fellowship for Y.M. from Research Fellowships of Japan Society for the Promotion of Science for Young Scientists is also gratefully acknowledged. C.Z. is a recipient of the Bristol-Myers Squibb Fellowship in Synthetic Organic Chemistry. We thank Mr. Surin K. Mong, Dr. Andrea Adamo, and Dr. Kyle A. Totaro for insightful discussions. We acknowledge the Biological Instrument Facility of MIT for providing access to the Octet Biolayer Interferometry System (NIH S10 OD016326) and to CD spectrometry (NSF-0070319). We also thank Prof. R. John Collier for providing essential laboratory equipment.

REFERENCES

(1) Szumski, M.; Buszewski, B. *J. Sep. Sci.* **2004**, *27* (10−11), 837.
(2) Dwivedi, P.; Bendiak, B.; Clowers, B. H.; Hill, H. H. *J. Am. Soc. Mass Spectrom.* **2007**, *18* (7), 1163.
(3) Simons, K.; Toomre, D. *Nat. Rev. Mol. Cell Biol.* **2000**, *1* (1), 31.
(4) Kreil, G. *Annu. Rev. Biochem.* **1997**, *66*, 337.
(5) Soyez, D.; Toullec, J. Y.; Ollivaux, C.; Géraud, G. *J. Biol. Chem.* **2000**, *275* (48), 37870.
(6) Luo, L.; Kohli, R. M.; Onishi, M.; Linne, U.; Marahiel, M. A.; Walsh, C. T. *Biochemistry* **2002**, *41* (29), 9184.
(7) Anil, B.; Song, B.; Tang, Y.; Raleigh, D. P. *J. Am. Chem. Soc.* **2004**, *126* (41), 13194.
(8) Bang, D.; Makhatadze, G. I.; Tereshko, V.; Kossiakoff, A. A.; Kent, S. B. *Angew. Chem., Int. Ed.* **2005**, *44* (25), 3852.
(9) Werle, M.; Bernkop-Schnurch, A. *Amino Acids* **2006**, *30* (4), 351.
(10) Peeters, T. L.; Macielag, M. J.; Depoortere, I.; Konteatis, Z. D.; Florance, J. R.; Lessor, R. A.; Galdes, A. *Peptides* **1992**, *13* (6), 1103.
(11) Roda, O.; Valero, M. L.; Peiro, S.; Andreu, D.; Real, F. X.; Navarro, P. *J. Biol. Chem.* **2003**, *278* (8), 5702.
(12) Grieco, P.; Balse, P. M.; Weinberg, D.; MacNeil, T.; Hruby, V. J. *J. Med. Chem.* **2000**, *43*, 4998.
(13) Roth, A. L.; Marzola, E.; Rizzi, A.; Arduin, M.; Trapella, C.; Corti, C.; Vergura, R.; Martinelli, P.; Salvadori, S.; Regoli, D.; Corsi, M.; Cavanni, P.; Calo, G.; Guerrini, R. *J. Biol. Chem.* **2006**, *281* (30), 20809.
(14) Ramalingam, K.; Eaton, S. R.; Cody, W. L.; Lu, G. H.; Panek, R. L.; Waite, L. A.; Decker, S. J.; Keiser, J. A.; Doherty, A. M. *Bioorg. Med. Chem.* **1995**, *3* (9), 1263.
(15) Braisted, A. C.; Wells, J. A. *Proc. Natl. Acad. Sci. U. S. A.* **1996**, *93* (June), 5688.
(16) Werle, M.; Schmitz, T.; Huang, H.-L.; Wentzel, A.; Kolmar, H.; Bernkop-Schnürch, A. *J. Drug Target.* **2006**, *14* (3), 137.
(17) Kolmar, H. *Curr. Opin. Pharmacol.* **2009**, *9*, 608−614.
(18) Wentzel, A.; Christmann, A.; Krätzner, R.; Kolmar, H. *J. Biol. Chem.* **1999**, *274* (30), 21037.
(19) Lahti, J. L.; Silverman, A. P.; Cochran, J. R. *PLoS Comput. Biol.* **2009**, *5* (9), e1000499.
(20) Kimura, R. H.; Jones, D. S.; Jiang, L.; Miao, Z.; Cheng, Z.; Cochran, J. R. *PLoS One* **2011**, *6* (2), e16112.
(21) Moore, S. J.; Cochran, J. R. *Methods Enzymol.* **2012**, *503*, 223.
(22) Moore, S. J.; Hayden Gephart, M. G.; Bergen, J. M.; Su, Y. S.; Rayburn, H.; Scott, M. P.; Cochran, J. R. *Proc. Natl. Acad. Sci. U. S. A.* **2013**, *110* (36), 14598.
(23) Williams, J. A.; Day, M.; Heavner, J. E. *Expert Opin. Pharmacother.* **2008**, *9* (9), 1575.
(24) Guo, Y.; Sun, D.-M.; Wang, F.-L.; He, Y.; Liu, L.; Tian, C.-L. *Angew. Chem., Int. Ed.* **2015**, *54* (48), 14276.
(25) Imperiali, B.; Ottesen, J. J. *J. Pept. Res.* **1999**, *54*, 177.
(26) Grönwall, C.; Ståhl, S. *J. Biotechnol.* **2009**, *140* (3−4), 254.
(27) Fezoui, Y.; Weaver, D. L.; Osterhout, J. J. *Proc. Natl. Acad. Sci. U. S. A.* **1994**, *91* (9), 3675.
(28) Binz, H. K.; Amstutz, P.; Pluckthun, A. *Nat. Biotechnol.* **2005**, *23* (10), 1257.
(29) Chin, J. W.; Schepartz, A. *Angew. Chem., Int. Ed.* **2001**, *40* (20), 3806.
(30) Nord, K.; Gunneriusson, E.; Ringdahl, J.; Ståhl, S.; Uhlén M, N. P. *Nat. Biotechnol.* **1997**, *15* (8), 772.
(31) Nilsson, B.; Moks, T.; Jansson, B.; Abrahmsen, L.; Elmblad, A.; Holmgren, E.; Henrichson, C.; Jones, T. A.; Uhlen, M. *Protein Eng., Des. Sel.* **1987**, *1* (2), 107.
(32) Fujino, T.; Goto, Y.; Suga, H.; Murakami, H. *J. Am. Chem. Soc.* **2013**, *135* (5), 1830.
(33) Dedkova, L. M.; Fahmi, N. E.; Golovine, S. Y.; Hecht, S. M. *J. Am. Chem. Soc.* **2003**, *125* (22), 6616.
(34) Le-Nguyen, D.; Nalis, D.; Castro, B. *Int. J. Pept. Protein Res.* **1989**, *34* (6), 492.
(35) Krätzner, R.; Debreczeni, J. E.; Pape, T.; Schneider, T. R.; Wentzel, A.; Kolmar, H.; Sheldrick, G. M.; Uson, I. *Acta Crystallogr., Sect. D: Biol. Crystallogr.* **2005**, *61* (9), 1255.
(36) Deisenhofer, J. *Biochemistry* **1981**, *20* (9), 2361.
(37) Nielsen, K. J.; Alewood, D.; Andrews, J.; Kent, S. B.; Craik, D. J. *Protein Sci.* **1994**, *3* (2), 291.
(38) Walewska, A.; Jaskiewicz, A.; Bulaj, G.; Rolka, K. *Chem. Biol. Drug Des.* **2011**, *77* (1), 93.
(39) Starovasnik, M. A.; Braisted, A. C.; Wells, J. A. *Proc. Natl. Acad. Sci. U. S. A.* **1997**, *94* (19), 10080.
(40) Erlanger, B. F.; Kokowsky, N.; Cohen, W. *Arch. Biochem. Biophys.* **1961**, *95* (2), 271.
(41) Durek, T.; Zhang, J.; He, C.; Kent, S. B. H. *Org. Lett.* **2007**, *9* (26), 5497.
(42) Simon, M. D.; Heider, P. L.; Adamo, A.; Vinogradov, A. A.; Mong, S. K.; Li, X.; Berger, T.; Policarpo, R. L.; Zhang, C.; Zou, Y.; Liao, X.; Spokoyny, A. M.; Jensen, K. F.; Pentelute, B. L. *ChemBioChem* **2014**, *15* (5), 713.
(43) Mong, S. K.; Vinogradov, A. A.; Simon, M. D.; Pentelute, B. L. *ChemBioChem* **2014**, *15* (5), 721.
(44) Colgrave, M. L.; Craik, D. J. *Biochemistry* **2004**, *43* (20), 5965.
(45) Zhang, Y.; Cougnon, F. B. L.; Wanniarachchi, Y. A.; Hayden, J. A.; Nolan, E. M. *ACS Chem. Biol.* **2013**, *8* (9), 1907.
(46) Pettersen, E. F.; Goddard, T. D.; Huang, C. C.; Couch, G. S.; Greenblatt, D. M.; Meng, E. C.; Ferrin, T. E. *J. Comput. Chem.* **2004**, *25* (13), 1605.
(47) Hess, B.; Kutzner, C.; van der Spoel, D.; Lindahl, E. *J. Chem. Theory Comput.* **2008**, *4*, 435.
(48) Jiang, F.; Wu, Y.-D. *J. Am. Chem. Soc.* **2014**, *136*, 9536.
(49) Jiang, F.; Zhou, C.-Y.; Wu, Y.-D. *J. Phys. Chem. B* **2014**, *118*, 6983.
(50) Louis-Jeune, C.; Andrade-Navarro, M. A.; Perez-Iratxeta, C. *Proteins: Struct., Funct., Genet.* **2012**, *80* (2), 374.
(51) Starovasnik, M. A.; Braisted, A. C.; Wells, J. A. *Proc. Natl. Acad. Sci. U. S. A.* **1997**, *94* (19), 10080.
(52) MacArthur, M. W.; Thornton, J. M. *J. Mol. Biol.* **1991**, *218* (2), 397.
(53) Reinwarth, M.; Avrutina, O.; Fabritz, S.; Kolmar, H. *PLoS One* **2014**, *9* (10), e108626.
(54) Gupta, K.; Kumar, M.; Balaram, P. *Anal. Chem.* **2010**, *82* (19), 8313.

DOI: 10.1021/jacs.6b03765
J. Am. Chem. Soc. 2016, 138, 12099−12111